Monte Carlo Simulation of Seismic Location Errors for Moving Vehicles

October 4, 2001

Roy J. Greenfield+ and M. L. Moran*
+Penn State University, State College, PA
*USACE ERDC-CRREL

ABSTRACT

A method was developed to predict the distribution of seismic source mislocation errors for tracked vehicles using bearing and range (r) location statistics obtained from field data. The method is of use for 1) guiding the design and deployment of seismic sensor networks and 2) statistically modeling seismic network tracking performance.

In the present work, a seismic array is composed of one or multiple seismic subarrays each of which makes estimates of bearing and range. The bearing and range estimates are taken to be normally distributed around the true target location with errors σ^b and σ^r respectively. When these σ's are used in our Monte Carlo simulation, we chose a true source point, and network geometry (array locations). Using these source and sensor positions, a set of true bearing and r are computed. The Monte Carlo simulation is done with 100 trials, in each trial a random error is added to the true bearing and r for each array according to the observed σ. For each of the 100 bearing and r Monte Carlo "measurements", a weighted least squares solution for the East and North value of the source is found. A statistical fit for all 100 trials is used to find the 90% confidence location ellipse surrounding the true source point.

Two types of displays are presented. The first fixes σ^b and σ^r and makes a map that displays the error ellipse axes and orientation as a function of map position. The second uses a fixed map position and displays the error ellipse axes and orientation as a function of σb and σr. This allows convenient analysis of how the location error changes with changes of the array measurement accuracy. The later format is particularly suited for evaluating the impact of seismic senor configuration on network tracking performance.

Results are presented for a number of different network configurations representative of battlefield situations. Both single array and multiple array networks are considered. The values used for σb and σr in these simulations were chosen by examining results from a number of past field test data sets.

Using field data it was found that subarrays with 11 or 12 vertical seismic sensors could get bearing with RMS errors on the order of 5°. Subarrays with only 3 or 4 sensors and diameters of 5 to 10 m gave similar errors. For small subarrays with 3 sensors in an equilateral triangle with legs of 1 m, scatter was below 10° but a significant bias existed; the bias might be removed by a calibration procedure.

Range was found from amplitude measurements at five sites. A model appropriate to the amplitude decay of a surface wave on lossy medium was fit to data. Several band passes were examined. RMS Range

Report Documentation Page

Report Date	Report Type	Dates Covered (from... to)
04 Oct 2001	N/A	-

Title and Subtitle Monte Carlo Simulation of Seismic Location Errors for Moving Vehicles	**Contract Number**
	Grant Number
	Program Element Number
Author(s)	**Project Number**
	Task Number
	Work Unit Number
Performing Organization Name(s) and Address(es) Penn State University USACE ERDC-CRREL State College, PA	**Performing Organization Report Number**
Sponsoring/Monitoring Agency Name(s) and Address(es) Department of the Army, CECOM RDEC Night Vision & Electronic Sensors Directorate AMSEL-RD-NV-D 10221 Burbeck Road Ft. Belvoir, VA 22060-5806	**Sponsor/Monitor's Acronym(s)**
	Sponsor/Monitor's Report Number(s)

Distribution/Availability Statement
Approved for public release, distribution unlimited

Supplementary Notes
See also ADM201471, Papers from the Meeting of the MSS Specialty Group on Battlefield Acoustic and Seismic Sensing, Magnetic and Electric Field Sensors (2001) Held in Applied Physics Lab, Johns Hopkins Univ, Laurel, MD on 24-26 Oct 2001. Volume 2 (Also includes 1999 and 2000 Meetings), The original document contains color images.

Abstract

Subject Terms

Report Classification unclassified	**Classification of this page** unclassified
Classification of Abstract unclassified	**Limitation of Abstract** UU

Number of Pages
16

errors for the five sites varied between 45 and 145 m. A curve was produced comparing amplitude versus range for the five sites. This demonstrates that a site's amplitude versus distance must be calibrated to estimate distance from amplitude.

1. INTRODUCTION

The major effort has been towards determining how accurately a continuous source of seismic signal, such as a tank, can be located from it's seismic emissions. The location of a source is a key piece of information for monitoring hostile movements.

A seismic location system is considered that is composed of a group of subarrays Each subarray has a number of individual seismic sensors. A typical subarray will have a diameter of a few meters to 40 meters. . All the subarrays will be termed an array.

This paper is divide into 3 sections: 1) RANGE ESTIMATION, 2) BEARING ESTIMATION, and 3) LOCATION ACCURACY. In the first two sections estimates are made of the range and bearing accuracy that can be obtained by processing past field test data. In the third section a method is developed an applied to estimate source location errors.

2. RANGE ESTIMATION

2.1. Method

The amplitude of a seismic signal decays because of geometric spreading and attenuation. The attenuation is due to inelastic losses and to scattering due to inhomogenaity. For a Rayleigh surface wave the amplitude dependence on distance is of the form

$$A = [\text{reference amplitude}][\text{geometric spreading}][\text{attenuation}]$$

$$= [A_0]\left[r^{-0.5}\right]\left[e^{-\frac{r\pi f}{Qc}}\right]$$

where

A_0 = reference amplitude

r = range

Q = quality factor

c = wave velocity

f = frequency

A linear least squares fit, for a and b, is done in the linear form

$$P_{dB} + 10\log(r) = a + br$$

where

$$a \equiv 10\log\left(A_0^2\right)$$

$$b = 10\log\left(e^{-\frac{2\pi fr}{Qc}}\right) = -20\pi f \log(e)/Qc$$

$P \equiv$ *power and* P_{dB} is the power in dB.

$$P_{dB} = 10\log(P)$$

The values of a and b are found by a linear least squares fit to minimize the form:

$$E^2(a,b) \equiv \sum_{i=1}^{Numb.Obs.} \left[P_{dB,i}^{Obs.} - P_{dB,i}^{Pred.}(a,b)\right]^2$$

$$= \sum_{i=1}^{Numb.Obs.} \left[P_{dB,i}^{Obs.} + 10\log(r) - (a+br)\right]^2$$

2.2. Results

Data from five of field tests were fit and used to estimate error in range estimation; the data designations are given in Table 1. An example of a range fit is shown in Figure 1. Fits were made over several different band passes.

Table 1. Data used in range fits and in bearing fits.

Designation	Data Used
Yuma, AZ	Yuma Proving Ground, Smart Weapons Test Range 9/14/200 Four wheel Drive; File 14,
Aberdeen, MD, Site 1	June 11, 1996, 10c runs, Piston Tank ; 10:18 34:42 53:55 58:64 72:79 92:97 105:118 % file vector
Ft. Greely, AK, Site 1	1/27/1997, , Piston Tank; 34:42 53:64 % file vector
Ft. Greely, AK, Site 2	Dec 11, 1997 ; File 56, , Piston Tank
Aberdeen, MD, Site 2	10/28/97 File84; File 56

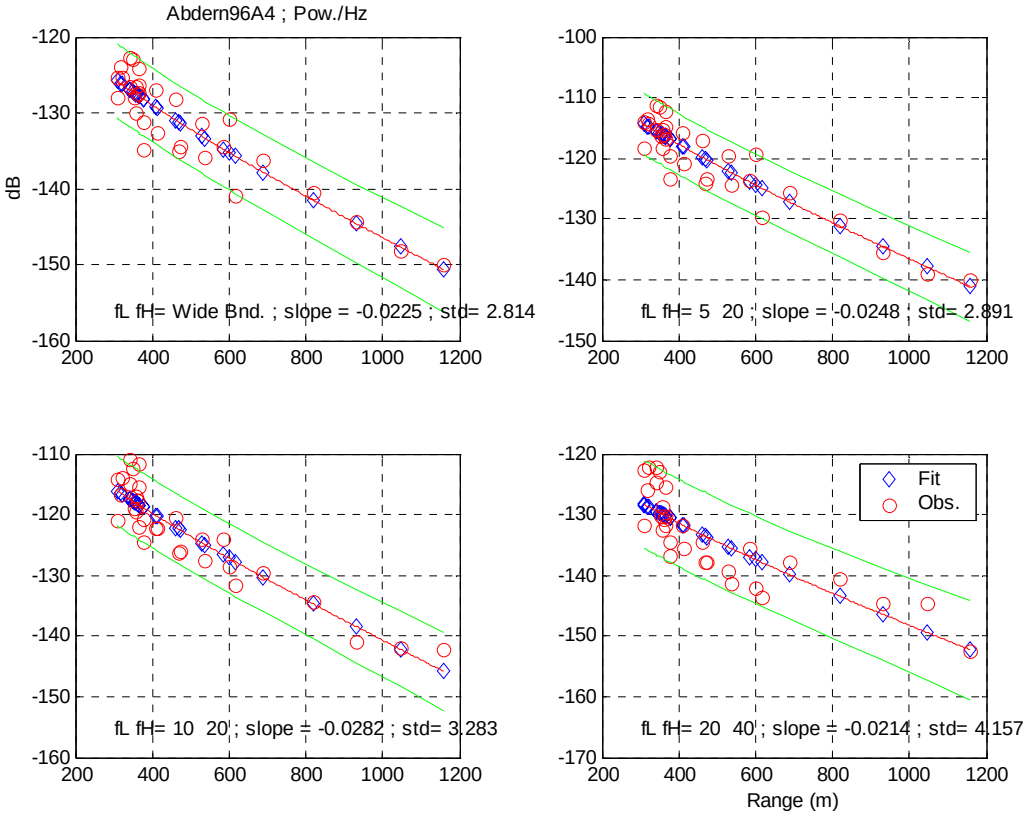

Figure 1. Fit to amplitude(Power/Hz) versus range data for Aberdeen, MD, Site 1. Band pass, slope, and Standard Deviation (std) are given on each panel.

After the a and b coefficients are found the range can be estimated from a power level measurement. Then for a group of observed power levels and GPS based range measurements (assumed to be correct) the standard deviation of the error in the estimated range is found. The error in range is defined as the predicted range minus the GPS range. The error in range that corresponds to the fit shown in Figure 1 is shown in Figure 1. Standard deviations of the range fit estimates for 5 sites are shown in Table 2.

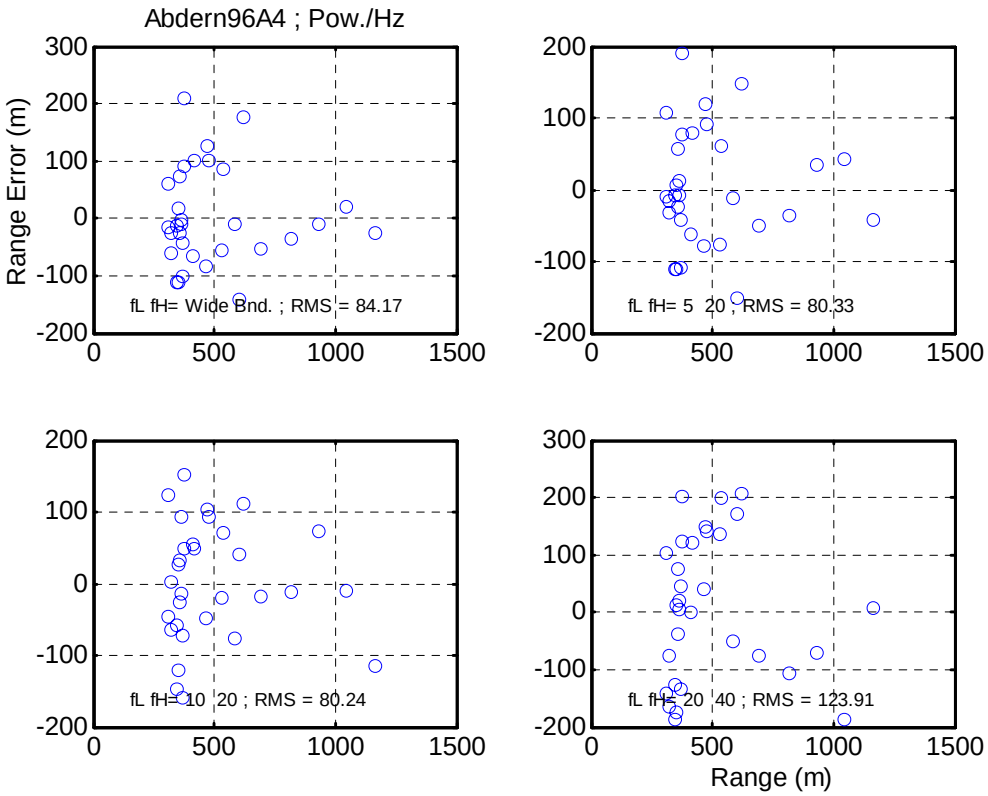

Figure 2. Range error versus range for data for Aberdeen, MD, Site 1 (see Table 1). Band pass and RMS error are given on each panel.

Table 2. Compilation of results for errors in range estimation. 10 to 20 Hz band

Data Set number	Location	Standard Deviation (m)	Range of Fit (m)
1	Ft. Greely Site 1	145	250-1500
2	Ft Greely Site 2	37	200-800
3	Aberdeen Stite1	80	350-1100
4	Aberdeen Site 2	64	110-350
5	Yuma, AZ.	40	100-320

2.3. Comparison of Amplitude for Different Sites

The fit to data for 5 different sites was complied on one plot, shown in Figure 2, to show the strong influence that geologic structure has on the amplitude versus distance curve. For each site the curve represents the fit to the data. The range of the plot indicates the range of the data used in the fit. There are large differences in amplitude levels and in the attenuation rate for the different sites. This indicates that some form of calibration must be done at a site if amplitude measurements are to be used to estimate range. The coefficients a and b are given in Tables 3 and 4.

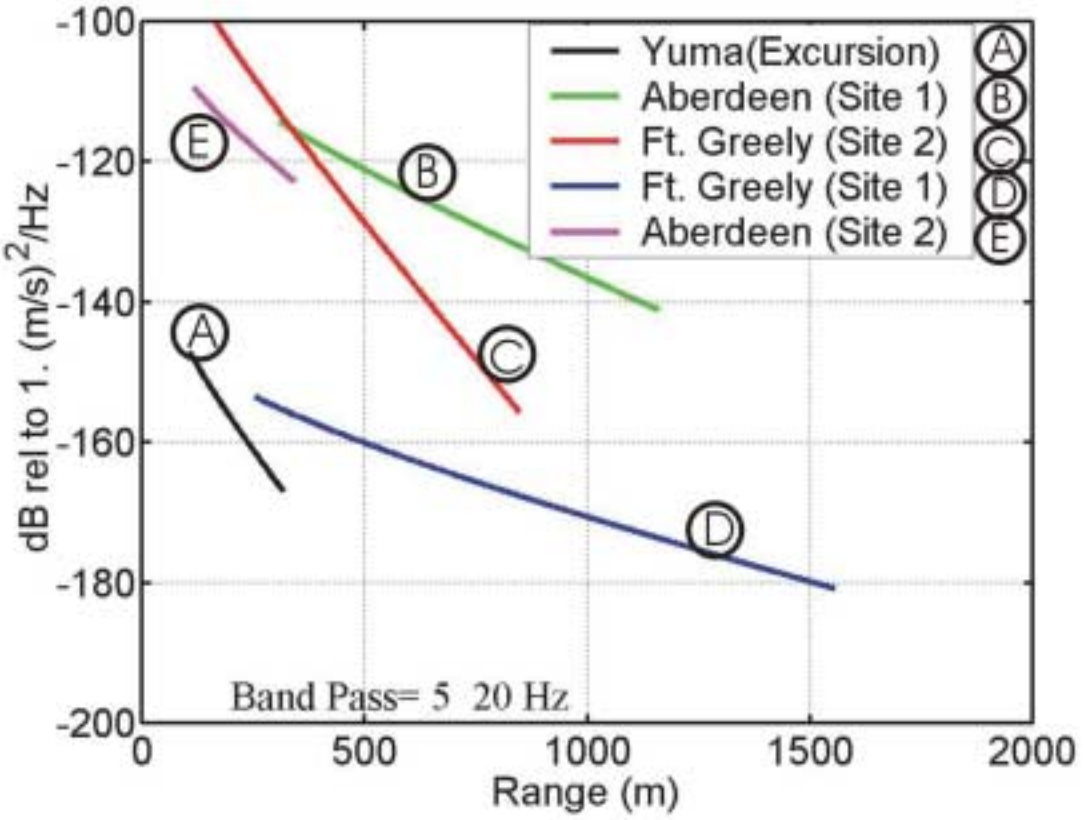

Figure 3 Amplitude versus distance for 5 sites. Shows strong effect of geology on amplitude. Lines extend over range of data used in fit. All sources were piston tanks except Yuma which was a Sports Utility Vehicle.

Table 3. Coefficient b.

	Wide Band	5-20 Hz	10-20 Hz	20-40 Hz
Yuma	-0.0787	-0.0717	-0.0732	-0.0926
Aberdeen, Site 1	-0.016282	-0.015713	-0.018326	-0.023465
Ft. Greely, Site 1	-0.022511	-0.024814	-0.028239	-0.021444
Ft. Greely, Site 2	0.0913	-0.0669	-0.0667	-0.0978
Aberdeen, Site 2	-0.044983	-0.033857	-0.048274	-0.089925

Table 4. Coefficient a.

	Wide Band	5-20 Hz	10-20 Hz	20-40 Hz
Yuma	-120.8522	-119.1978	-118.305	-113.7211
Aberdeen, Site 1	-93.9392	-81.7267	-82.4574	-96.7581
Ft. Greely, Site 1	-134.7292	-124.7725	-122.3322	-121.1379
Ft. Greely, Site 2	-63.0317	-68.164	-67.1417	-48.3767
Aberdeen, Site 2	-95.5133	-87.9894	-86.1321	-83.2409

2.4. Conclusions on Range Accuracy

- Data from 5 sites was analyzed.
- A form suited for surface wave amplitude versus distance with attenuation was used in the fits.
- A plot comparing the amplitude versus range for the five sites was given.
- Range error RMS for the sites varied between 40 and 145 m.

3. BEARING ESTIMATION

A study of bearing results was done to determine what accuracy can be expected from well populated seismic subarrays. This gives guidance on the variance to use in the simulation results section. In past work (e.g. Greenfield and Moran, 1997) looking at bearing determination for moving vehicles the subarrays were typically 12 to 30 m in diameter and had 12 geophones. A second purpose of this study is to look at the use of small arrays with limited numbers of sensors to see to what extent bearing determination deteriorates these smaller subarrays are used. To do this processing is done with 3 or 4 sensors selected from the full subarray. The past subarray collections were not done with this application in mind so the best small subarrays that could be formed from available data were used.

3.1. Method

Normal Frequency Wavenumber (fk) (e.g. Lacoss et. al., 1969) processing has given the most reliable and consistent results for determining bearing with subarrays and is used in all results presented.

3.2. Results

An example of bearing errors made with the three subarrays A, B, and C, shown in Figure 4, is shown in Figure 5. Subarray A was a large aperture, 40 m, subarray with 12 vertical geophones. It has been found in the past that this subarray gives accurate results. The smaller two subarrays had diameters up on the order of 15 to 20 m. The range to target was up to approximately 1,400 m. The bearing determination was done at 18 Hz. The mean phase velocity, estimated with subarray A, was 1850 m/s. A plot of the bearings determined by the subarrays are given in Figure 3; Figure 4 gives the bearing errors. Table 5 gives the errors found for the three subarrays. Errors > 12° were excluded. The bearing accuracy of the three subarrays was similar, with RMS errors of under 5°. The largest errors occur at the longest ranges which may be a signal to noise problem. Except for the bearings for ranges near 1500 m, there is no clear increase of error with distance. Bearing estimates were also done for data From Aberdeen site 1. The results are presented in Table 6.

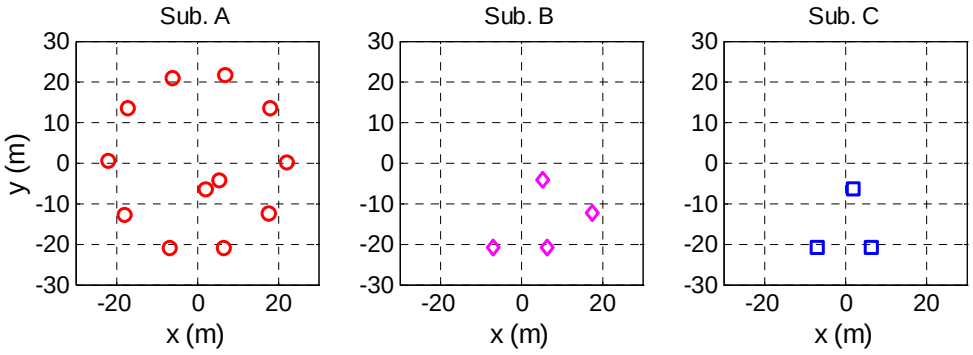

Figure 4. Subarrays for Ft. Greely data. A) is a typical subarray. B) and C) show small arrays formed by selected elements of A)

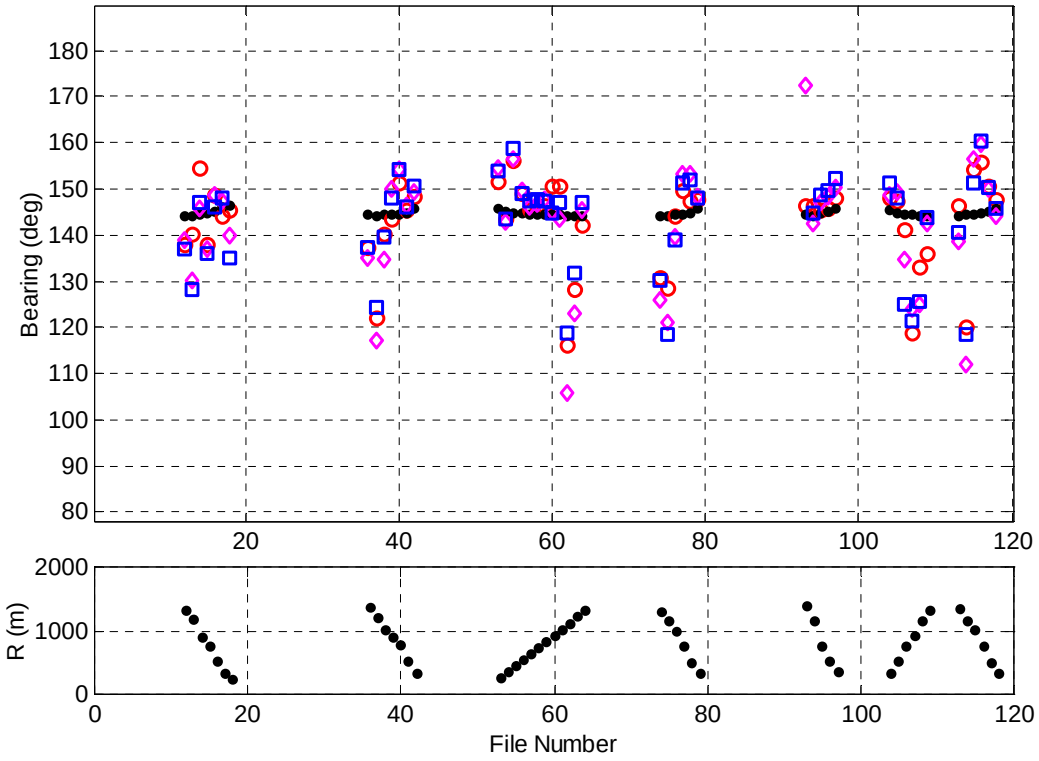

Figure 5. Top Ft. Greely, Jan 27, 1997 bearings determined with 3 subarrays. See Figure 4 to identify symbols. Small black dots indicate GPs bearing. Bottom shows range to tank source.

Table 5. Errors for Ft. Greely data of Figure 6.

subarray	mean error (°)	Standard Deviation (°)	RMS Error (°)
A	1.0934	4.6006	4.6855
B	0.7559	4.8745	4.8812
C	1.1633	4.4129	4.517

Table 6. Errors for Aberdeen site 1.

subarray	Diameter (m)	Number of geophones	mean (°)	Std (°)	RMS (°)
A	**20**	**12**	**-1.5468**	**5.3389**	**5.5349**
B	**10**	**4**	**-2.897**	**6.8006**	**7.3631**
C	**10**	**4**	**-3.1525**	**6.9962**	**7.6443**
D	**5**	**3**	**6.2212**	**8.839**	**10.7744**

3.3. Conclusions on Bearing estimation

- Data from 2 sites was used to estimate bearing error.
- Bearings obtained were compared to GPS.
- Subarrays with approximately 12 sensors gave RMS bearing error on the order of 5°.
- Small subarrays with 3 and 4 sensors with diameters of 5 to 10 m gave similar errors.
- Data from a third site, Yuma AZ was used. Very small subarrays with 3 sensors and diameters on the order of 1 m gave constant bearings, but in some cases the bearings had large biases. These biases might be correctable by careful planting, or sensor calibration.

4. LOCATION ACCURACY

4.1. Method

The location estimate (x, y coordinates) is found from the estimated bearing and range from a set of subarrays. The criteria used is the non-linear minimization of the weighted least squares error. The method is called Chi-Square Fitting (Press et al, 1992, p 653-655). The quantity minimized is

$$X^2(x,y) = \sum_{i=1}^{N}\left(\frac{\beta - \hat{\beta}(x,y)}{\sigma_i^b}\right)^2 + \sum_{i=1}^{N}\left(\frac{r - \hat{r}(x,y)}{\sigma_i^r}\right)^2$$

where

$x, y \equiv$ location positions

$X^2(x,y) \equiv$ CHI squared function to be minimized

$N \equiv$ number of stations

$\beta \equiv$ observed bearing (1)

$\hat{\beta}(x,y) \equiv$ predicted bearing

$\sigma_i^b \equiv$ square root of the variance of bearing i measurement

$r \equiv$ observed range

$\hat{r}(x,y) \equiv$ predicted range

$\sigma_i^r \equiv$ square root of the variance of range i measurement

The minimization is implemented to find x and y from a set of observations using the Matlab function **lsqnonlin.m**

4.2. Simulation Procedure for a error confidence ellipse map

An checkerboard grid of true source points is chosen A location determination error ellipse is simulated with the steps described in Table 7. Then the error ellipse is plotted at each true source point. A map is made for the grid of source points. The program **MapE.m** does this procedure.

Table 5. Procedure for producing an error ellipse

1	select array configuration	
2	select true x and y	
3	select σ for range and bearing	
4	generate true bearing and range	
5	use a Normal Distribution random number generator for error in bearing	
6	use a Normal Distribution random number generator for error in range	

7	add error in bearing to true bearing to get observed bearing	
8	add error in range to true bearing to get observed range	
9	fit for x and y using X^2 criteria (the variances used in the random number generation are used in the fit)	
10	repeat steps 5 to 9 M times	
11	fit the M locations found with an error confidence ellipse	
12	plot the axes of the error confidence ellipse on map	

Figure 6 illustrates how the scatter of estimates of the source point are fit by an ellipse and the axes of the ellipse are plotted for each true source point. A color code is used to allow a wide range of ellipse sizes to be plotted on the same figure. In black and white the color code does not show up so a few ellipse axes have been labeled.

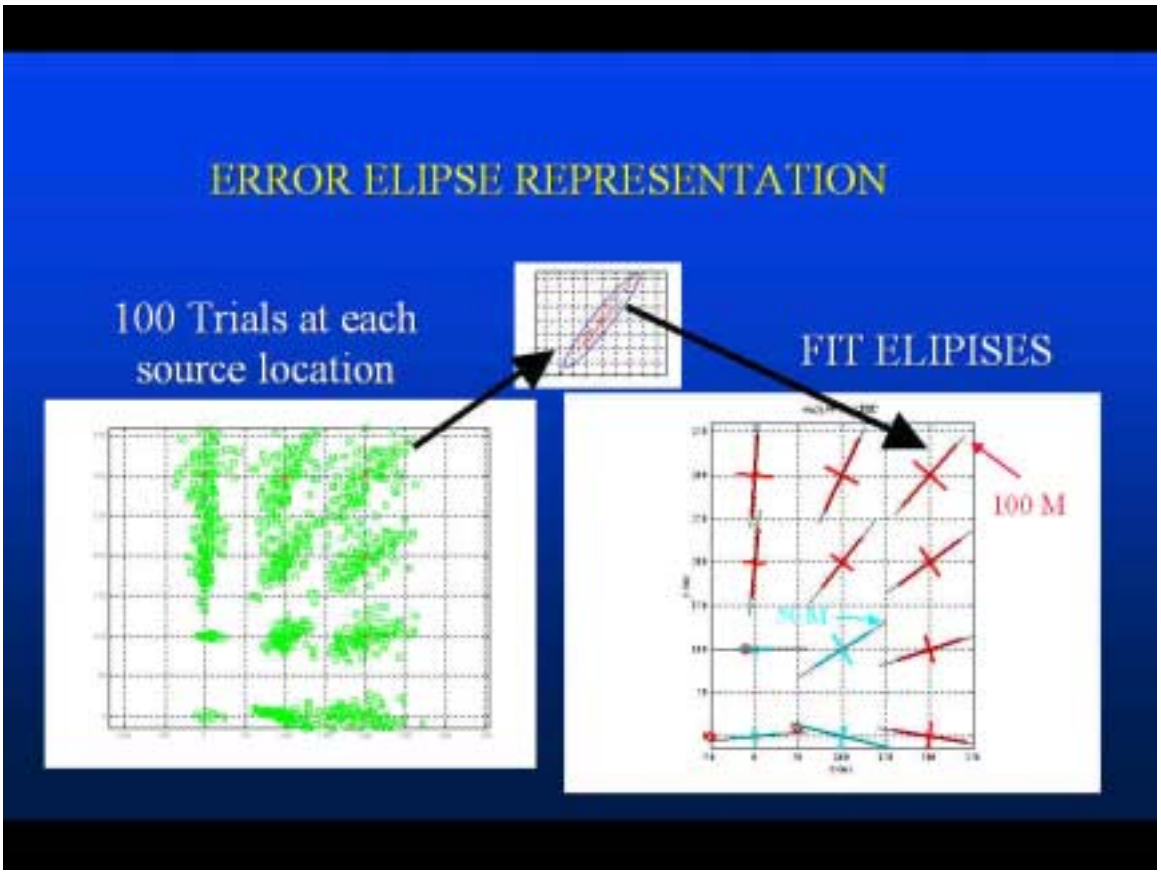

Figure 6. Formation of error ellipse maps. Green dots in left panel show individual locations scattered around true location. Small figure shows fit of ellipse to the individual locations. Semi-

major and semi-minor axis of ellipse is drawn at true location. Thin black line is length of the semi-major axis of maximum for the color.

For **MapE.m** the values of σ^b and σ^r can be functions of range. In the present implementation σ^b is treated as constant with range. σ^r is taken in the form

$$\sigma^r \equiv \begin{cases} \sigma_0 & r < r_0 \\ \sigma_0\left[1+\left(r - r_0\right)S'\right] & r >= r_0 \end{cases}$$

A program was also written to explore how location accuracy at a fixed map point varied with errors. For this program **VaryErr.m** the values of σ^b and σ^r are given as single values for the map point.

4.3. Results

An example of an error map is given in Figure 7. On these maps color is used as a scaling key, so in black and white the length of some of the axes are not clear, thus a few numbers have been added.

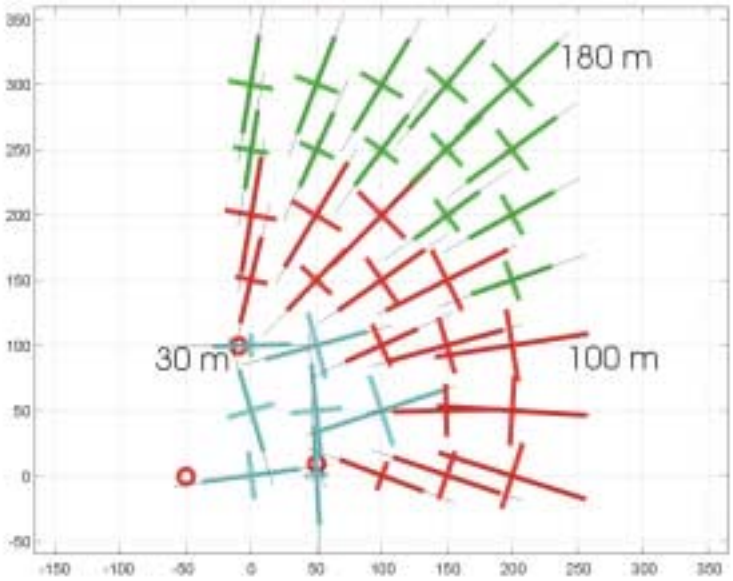

Figure 7. Error ellipse map for three subarrays (circles) . r_0=80 m; σ_0= 40 m; S=.01 (1/m); $\sigma_{Bear.}$ = 8°. Circles show the 5 subarray locations. The numbers indicates semi-major error ellipse axis. Horizontal axis is East, Vertical North.

Figure 8 show the way the error ellipse varies with σ^b and σ^r for a point

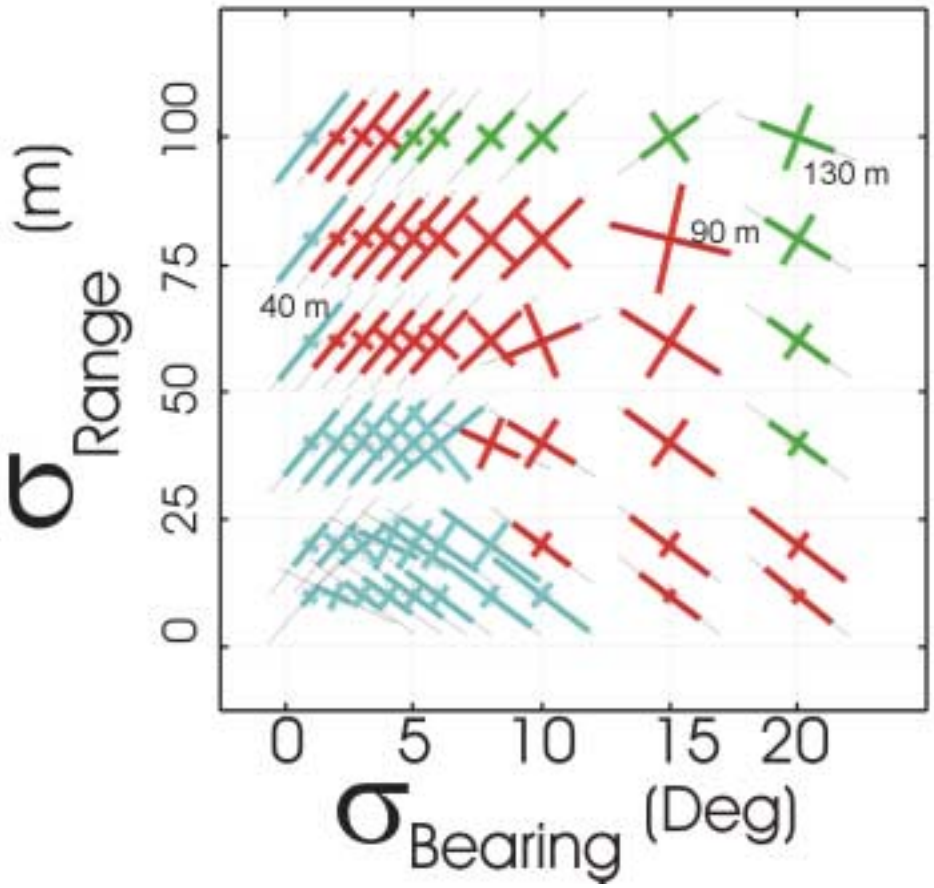

Figure 8. Error ellipse dependence on $\sigma_{Bearing}$ and σ_{Range}. Same three subarray configuration as previous figure. Source location at 200 East, 300 North. Horizontal axis is East, Vertical North. The numbers indicates semi-major error ellipse axis.

4.4. Conclusions on statistical modeling of source location error

- A weighted least squares method was developed to fit for source location using bearing and range estimates from one or more subarrays.
- The method was applied to synthetic data, with known error distributions.
- Maps giving 90% error ellipses were produced for a number of reasonable array configurations. Errors variances used were consistent with values found from past field test data.
- A presentation was developed to illustrate the dependence of the 90% error ellipses on the range and bearing error variances.

5. REFERENCES

Lacoss, R. T., Kelly, E. J. and Toksoz, M. N., 1969, Estimation of seismic noise structure using arrays : Geophysics, Soc. Of Expl. Geophys., **34,** 21-38.

Greenfield, R.J., and M.L. Moran, 1997, Seismic and acoustic observation of vehicle signals under summer and winter conditions: Proc. 5th Battlefield Acoustics Symposium, Ft. Meade, Md. 91-114.

Press, W. H., S. A. Teukolsky, W. T. Vetterling, and B. P. Flannery, 1992, "Numerical Recopies in Fortran", 2nd ed., Cambridge.

6. ACKNOWLEDGEMENTS

This work was supported by the US Army Office of the Program Manager for Mines, Countermines, and Demolitions in support of Hornet, Raptor, and Rattler-Track3 under MIPR1FPIC00544 and MIPR1APIC0051. Additional funding was provided by the US Army Corps of Engineers, Engineering Research and Development Center, Cold Regions Research and Engineering Laboratory (ERDC-CRREL) under PE62784/AT42. Work at Pennsylvania State University was supported by contract DACA89-99-C-0001 with ERDC-CRREL.